

Load bearing and deformation behavior of unreinforced and reinforced working platforms for mobile construction machines - new findings from field and model experiments

Rainer Worbes & Christian Moormann

Institute for Geotechnical Engineering, University of Stuttgart, Germany

ABSTRACT: Variety of construction projects, such as the erection of wind turbines and the production of deep foundations requires the use of heavy machinery on soft and unsustainable surfaces. Temporary working platforms in the form of on-poured and compacted, partially with geosynthetics reinforced earthworks are created here. In this context, there is an urgent need for optimization, since often the requirements of construction machinery are not correlated with the prepared work platforms and for the design of such temporary work platforms from unreinforced and reinforced base courses there are currently no generally accepted technical regulations. Within the framework of the research project "Supporting Layers for Working Platforms for Mobile Construction Machinery and Crane surfaces" at the Institute for Geotechnical Engineering of the University of Stuttgart, the load-bearing mechanism of reinforced and unreinforced base courses and the complex interaction between construction machine and subsoil will be investigated by a combination of field and model experiments with numerical simulations.

Keywords: supporting layer, working platform, geogrid reinforcement, machine-soil interaction

1 INTRODUCTION

For the use of heavy mobile construction machinery such as rotary or trench wall devices, rams, vehicle and crawler cranes, temporary working platforms are often created on site in the form of on-poured and compacted granular base structures. For better economical usage of the granular base material and higher bearing capacity, these working platforms are often reinforced with geosynthetics in form of geogrids and nonwovens. Especially for heavy mobile construction machines, which are mainly used for the creation of deep foundations and the construction of wind power plants, the bearing capacity of the upcoming subgrade is often insufficient for a safe and usable installation under consideration of all relevant operating and loading conditions. The use of working platforms and their correct dimensioning are therefore of central importance for the structural safety of the construction machinery and thus for the working safety. In this context, there is a need for optimization, since often the requirements of mobile construction machinery are not correlated with the prepared working platforms, because there are no generally accepted technical rules available for dimensioning of temporary working platforms made from unreinforced and reinforced aggregate layers. Aim of the research project, initiated by the Institute of Geotechnical Engineering of the University of Stuttgart is therefore the development of a design approach, to guarantee a safe operation of mobile construction machines under site conditions. The research strategy is based on experimental and numerical investigations. The numerical simulation models are validated with measured data obtained from large-scale model tests and field tests of unreinforced and reinforced base course systems. Based on numerical parameter studies, influences from geometric and geotechnical parameters are quantitatively investigated to gain an improved understanding of the load-bearing and deformation behavior of base course systems.

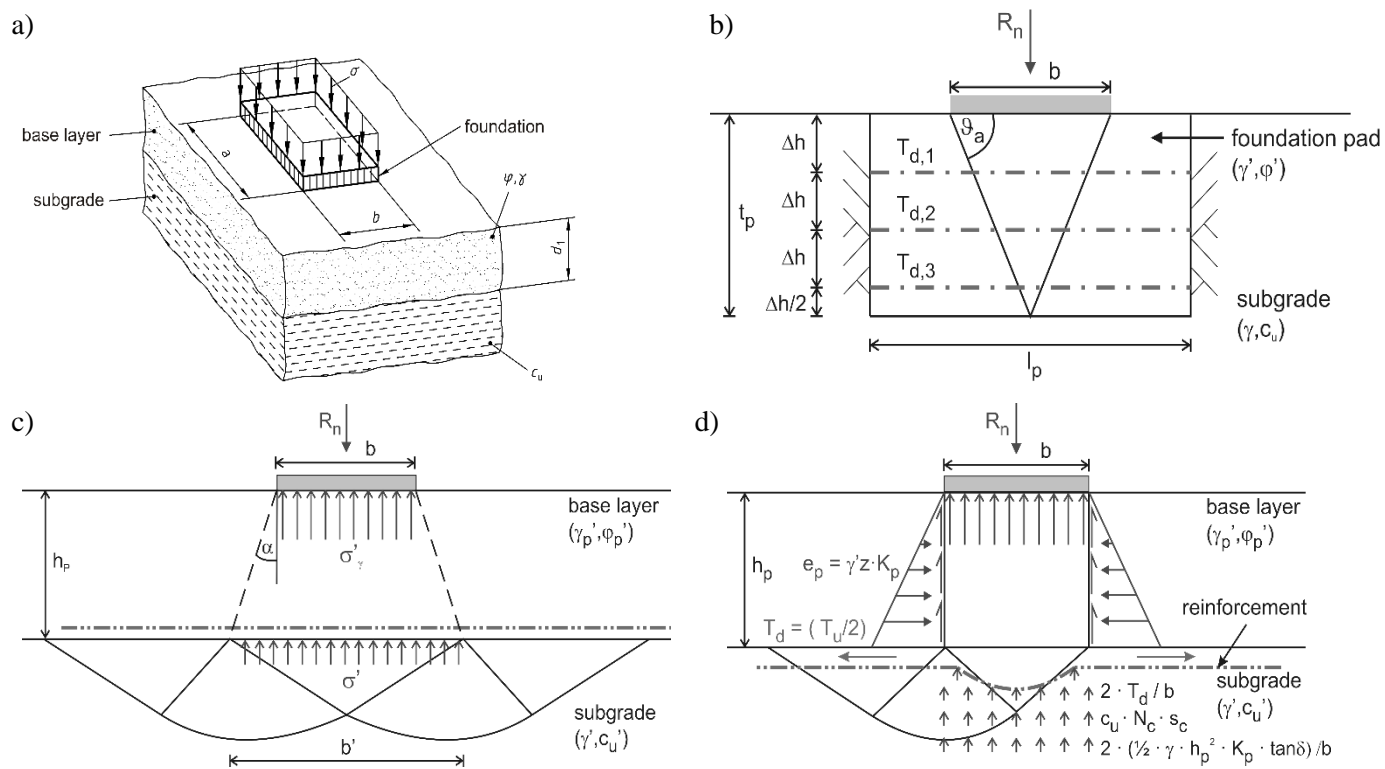


Figure 1. Design approaches after DIN 4017 – Appendix B (a), EBGEO (b), Giroud & Nioray (c) and Meyerhof according to BRE 470 (d).

2 ANALYTICAL DESIGN APPROACHES FOR UNREINFORCED AND REINFORCED SUPPORTING LAYERS

For the dimensioning of unreinforced and reinforced working platforms, various approaches for determining the bearing capacity of two-layer systems made of supporting and soft layer are available in the literature. These are mainly based on the principle of load distribution or load reduction on the underlying subgrade. In this case, the assumption is made that the thickness of the supporting layer and the shear strength have been chosen in such way, that the base failure occurs exclusively in the soft layer. After application of these approaches for load distribution due to the bearing layer, the bearing capacity of the subgrade is determined with the resulting vertical stresses. In some design methods, the required bearing layer thickness can be calculated directly.

2.1 Design approach according to German Standard DIN 4017 – Appendix B

The only standardized assessment approach for unreinforced base courses in Germany, is the dimensioning procedure for punching shear failure according to DIN 4017 Annex B [2] in Figure 1-a. The base layer hereby is considered by a combination of silo and bearing capacity theory. The main disadvantages of this analytical approach are the restrictions regarding the maximum base layer thickness and the lack of opportunity to consider the load bearing effect of geosynthetic reinforcements.

2.2 Design approach after EBGEO

A widespread design approach is the EBGEO with the approach shown in Figure 1-b for the dimensioning of reinforced foundation pads, which approximately correspond to the system of temporary working platforms. In this case, the bearing capacity is determined analogously to the German Standard DIN 4017. By using this approach influence of the aggregate layer and the geogrid are considered corrective factors due to the inhomogeneity of the ground. Disadvantage for the use for dimensioning working platforms is the limitation to a minimum number of two reinforcement layers with the same vertical distance between each layer, the maximum distance between each layer and the minimum distance to the subgrade.

2.3 Design approach after Giroud & Nioray

Figure 1-c shows the approach according to Giroud & Noiray (1981), which applies a load distribution in the support layer and thus achieves a vertical stress reduction on the soft layer. This approach was originally developed as a mechanical-empirical design method for unpaved roads reinforced with geosynthetics. The influence of the bearing behavior of geosynthetics is considered by assuming an additional tensile membrane effect depending on the maximum allowed rut depth.

2.4 Design approach after Meyerhof (BR 470)

A further possibility is the design approach by Meyerhof (1974) shown in Figure 1-d, where the supporting layer is considered by friction in the vertical shear surface. The frictional force results here from the passive earth pressure, which is inclined by the wall friction angle δ causing a reduction of the stress in the subgrade directly below the loading surface. The BR 470 from Directive of the British Research Establishment (2004/2007) is based on the design approach after Meyerhof and integrates it into a design method for self-propelled tracked working machines. This design method allows the dimensioning of unreinforced, as well as reinforced working platforms. The bearing capacity of geosynthetics is taken into account in a very simplified manner by considering an additional vertical reduction of the stress on the subgrade due to the tensile membrane effect.

2.5 Comparison between the different design approaches

The comparison of results from the different design approaches according to Kleih et. al. (2009), shows, huge differences between the results for the same design situation. While the approaches according to Meyerhof and DIN 4017 - Appendix B are more likely to underestimate the load bearing capacity, the results according to EBGeo and Giroud & Nioray provide similar values. It is not clear to the user which of these design approaches is suitable for the safe dimensioning of working platforms for mobile construction machines.

3 LARGE-SCALED MODEL TESTS

3.1 Experimental Concept

The geotechnical model tests are carried out as 1-g tests on a 1:3 scaling. Figure 3-a illustrates the geometry and the arrangement of the sensors in the experiment. The basal area of the test field is 4.82 m x 2.72 m, in which two model tests can be conducted separately from each other. Each test field has the dimensions 2.41 m x 2.72 m. The subgrade, represented by a layer of loess loam (SC/CL classification according to USCS) with an undrained shear strength of 20 kN/m², has a height of 0.80 m. The shear strength c_u of the soft layer can be varied from 10 kN/m² to 30 kN/m². The soil parameters of the densified loess loam are controlled by the moisture content and the undrained shear strength is measured by in-situ vane shear tests. Above the soft layer, an aggregate layer is installed with a thickness of 0.20 m, which can be varied from 0.10 m to 0.30 m. For the installation of the bearing layer a well-graded sand-grit mixture with a grain size between 0 mm and 16 mm is used. The gravel mixture is incorporated with a proctor density of $D_{Pr} = 100\%$. The size of the load plate is 35 cm x 25 cm (l x b), and the vertical test load is applied with an eccentricity $e = 0.04 \times b = 1$ cm relative to the shorter foundation side to provide the direction of the basic fracture. Deformations on the surface are measured by potentiometric distance sensors (LVDT) at nine points. In the reinforced test, the strains in the geogrid are additionally measured at seven points by strain gauges. In the unreinforced test, a nonwoven is used as a separating element between the soft layer and the supporting layer. It can be assumed that that the nonwoven membrane has no significant reinforcement function. For the reinforcement a composite product made of a biaxial geogrid (laid, welded knots) with a maximum tensile strength of 30 kN/m and a biaxial tensile stiffness of $J_{0-2\%} = 600$ kN/m combined with a nonwoven was used. This composite product has also been placed between the soft layer and the bearing layer fulfilling both the functions of reinforcing and separating.

3.2 Loading Scheme

The loading scheme, shown in Figure 3-c can be divided in three stages. The first stage is the monotonous loading phase in which the load is initially increased to the average cyclic load with a velocity of 0,1 kN/s. This

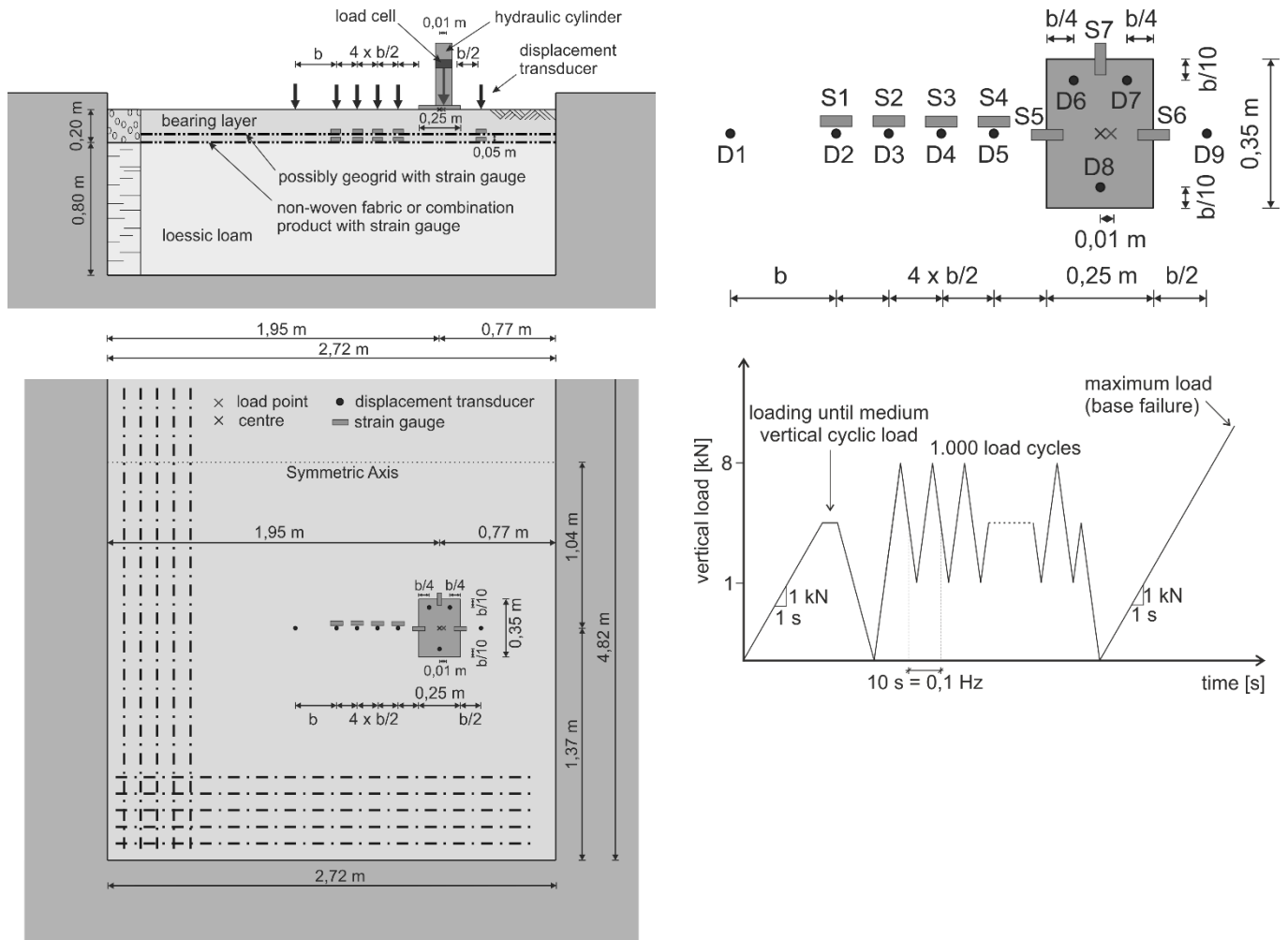


Figure 3: Setup and dimensions of the performed model tests (a), arrangement of the potentiometric distance sensors (LVDT) and the strain-gauges on the geogrid around the load plate (b) and load concept with three stages: initial loading, cyclic loading and maximum loading (c).

causes plastic deformations prior to the cyclic loading stage and gives information about the initial stiffness. After that, the relief starts and the second stage, the cyclic loading, which simulates load effects under operating conditions begins. In this stage 1,000 load cycles with a frequency of 0.1 Hz and the amplitude of 3.5 kN between 1 kN and 8 kN were applied. During the final stage, the load is increased up to a defined failure state, in order to obtain the bearing capacity of the base course system.

3.3 Testing Results

In the following chapter, the results of the unreinforced and reinforced test are presented and compared to analyze the influence of the geogrid reinforcement. Figure 4 shows the deformation of the load plate during the cyclic loading of the unreinforced and the reinforced base course. The deformation is locally limited and the steel plate punches into the base course. The unreinforced base layer deforms much stronger during the first load cycles, with no obvious difference in the accumulation of permanent deformations during cyclic loading. The settlement of the load plate has almost doubled in both systems after 1,000 load changes compared to the initial load. Figure 5 shows the comparison of the load-settlement curves between the unreinforced and the reinforced bearing layer system for the static load applied after the cyclic loading phase. Up to almost 16 kN, the rigidity of both two-layer systems is comparatively high and there is almost a very small increase in the deformation. The main reason for this is the compression caused by the cyclic preload with a maximum load of 8 kN. At around 56 kN, the load plate is relieved due to the maximum press stroke in the unreinforced system. The relief shows high plastic deformation of 15 cm. The plate is then loaded again and reaches the failure load at 67.6 kN. With increasing load the difference between both systems becomes more significant, due to the activation of the Geogrid reinforcement and the tensile membrane effect. The influence of this effect is locally limited to a range of about 1.5b around to the load plate, due to the punching of the load plate into the weak sub layer.

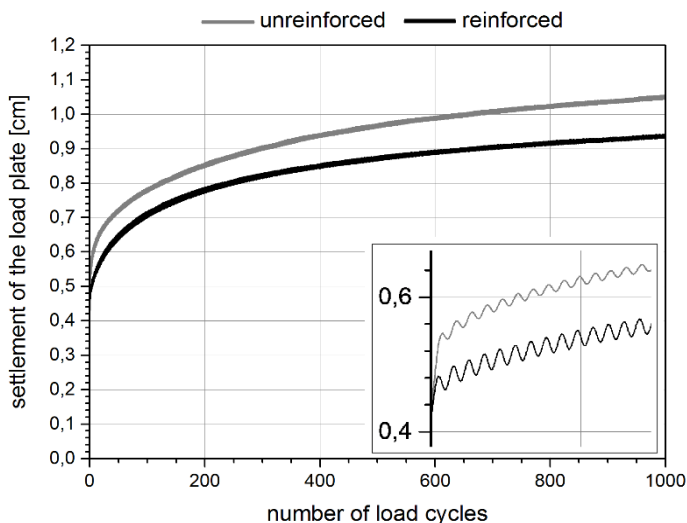


Figure 4. Comparison of the settlement of the load plate on the reinforced and unreinforced support layer for cyclic loading.

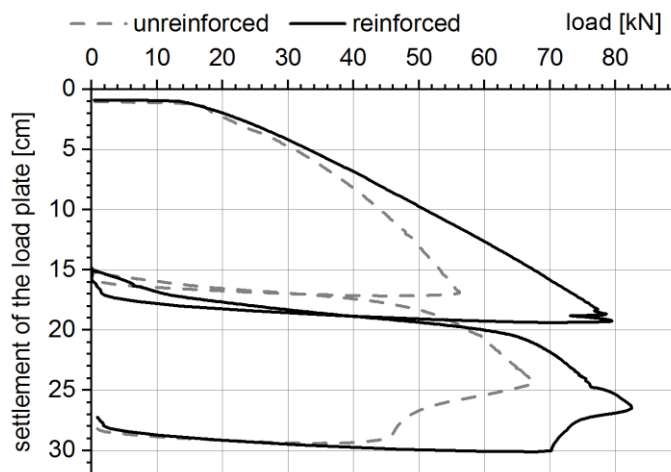


Figure 5. Comparison of the settlement of the load plate on the reinforced and unreinforced support layer for maximum loading.

3.4 Failure Mechanism

The failure mechanism consists of a combination of punching shear in the bearing layer and the base failure of the subgrade. In case of the unreinforced system, base failure takes place after perforation of the supporting layer. Due to the low shear strength of the soft layer, there exists no general shear failure and the system changes to a punching shear failure with increasing deformations. For the reinforced system both mechanisms, the perforation of the supporting layer and the punching shear failure take place long before the reinforcement fails. The final failure state, from which no further increase of the vertical load is possible, is marked by the rupture of the geogrid. The geogrid used in the test rips under the edge of the load plate, due to the increasing tensile forces in this area.

4 MEASUREMENT OF THE LOAD-BEARING AND DEFORMATION BEHAVIOR OF A GEOGRID REINFORCED WORKING PLATFORM IN A WINDPARK

To investigate the load-bearing and deformation behavior of base course systems under site conditions, field tests on real scale are an essential component of the research project. In the following chapter the results from the measurement of the load-bearing and deformation behavior of a geogrid reinforced working platform in a windpark in Rethwisch near Hamburg is presented. Additional to an existing working platform, a test field with the size of 20 m x 20 m was instrumented.

4.1 Experimental Setup

The subgrade in this area consists of an approximately 2.5 m thick organic soft layer, which is underlain by about 4.0 m of loose and silty sand. The soft layer consists mainly of silty peat, with a mean natural water content of $w_L = 230\%$. The peat thus has a very soft to pasty consistency. For the base layer made of crushed ballast material (0/63) a height of 0.90 m and a two-layer reinforcement with geosynthetics were provided. The lower reinforcement layer was placed between the subgrade and the aggregate layer and was reinforced with a combination product consisting of a nonwoven and a biaxial geogrid (laid with welded knots) with a short-term tensile strength of 60 kN/m. The upper layer was arranged 0.50 m above the subgrade, were an additional biaxial geogrid with the short term tensile strength of 40 kN/m was installed. The aggregate layer was compacted with a vibratory roller in two layers. Above the base layer was a crane mat arranged made from two-layered azobe wood beams aligned orthogonal to each other with the total dimensions of 6.0 m x 5.0 m and a total thickness of 0,40 m. The layer structure of the trial field and the arrangement of the measuring sensors are shown schematically in Figure 6. The crane mat was loaded with crane counterweights (4 x 10 t = 40 t / layer) with a total load burdened up to 280 t. Subsequently, the load was held for a time of about 80 min.

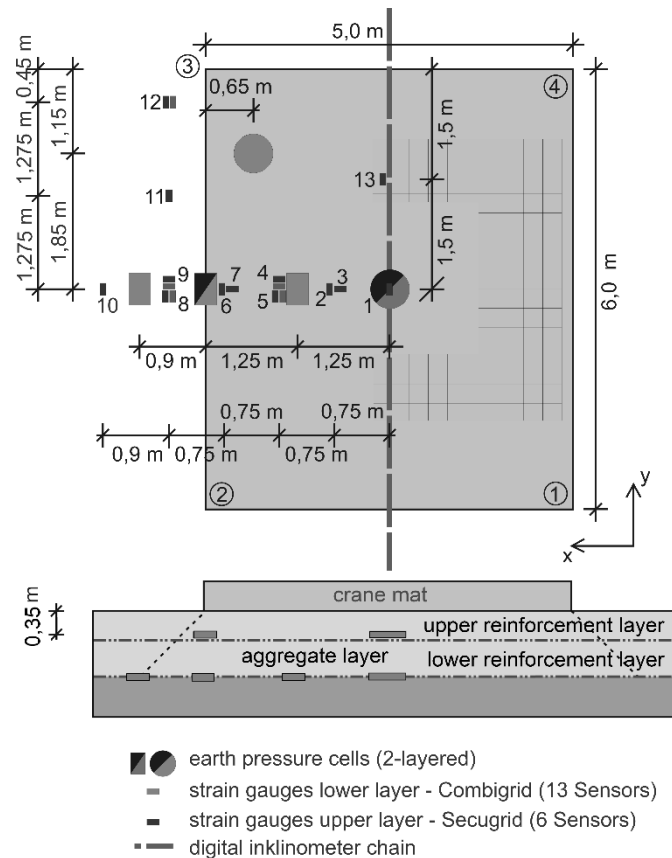


Figure 6. Setup and dimensions of the test field and arrangement of the sensor devices.

4.2 Measuring concept

For recording the stress and deformation states of the reinforced supporting layer different sensor types were used. The measuring sensors distributed on two measuring axes and two layers, focusing on the lower reinforcement layer. The strain of geogrid was recorded with linear film strain-gauges at 19 measuring points. These were directly applied on the longitudinal and transverse ribs of the geogrid. To compensate strain from bending deformation and temperature changes, each measuring point was used as a full-bridge with four single strain gauges for each point. To protect the strain gauges against moisture, excessed pore water, mechanical damage and groundwater, these were added with sealant and an adhesive film. For measuring the total vertical earth pressure and to assess the load distribution within the base course a total of seven earth pressure transducers were installed. The lower layer was directly installed on the height of the lower geogrid layer. The earth pressure transducers in the upper layer were installed about 0.35 m below the surface of the base layer and thus allow an estimation of the vertical stress induced from the crane mat. To ensure consistent stress on the surface of the earth pressure cells and to minimize measurement inaccuracies these were embedded with fine quartz sand. For measuring the settlement in the soft layer a digital inclinometer chain was used, which was installed below the interface between base layer and subgrade.

4.3 Results

Figure 8 shows the results of measuring points 3, 5, 7 and 9 along the main measuring axis for both the upper and the lower layer. It can be clearly seen that the strains in both layers increase disproportionately up to the maximum load of 280 t and reach their maximum values at the edge of the crane mat. This results from the punching shear failure of the crane mat, which greatly increases the elongation of the geogrid reinforcement in this area. The strains in the lower layer continue to increase even after reaching the maximum load due to consolidation. Due to the stress concentration and the relatively stiff crane mat, the strains at the edges increase more strongly with increasing load, which is additionally increased by tilting of the whole crane mat and counterweights. This is mainly due to the consolidation of the soft layer, which causes a further punching of the crane mat into the supporting layer. The further sinking of the crane mat, however, causes a further stress and strain concentration at the edge. After relieving, large plastic expansion parts still remain in the geogrid resulting from the stress due to the deformation-induced activation. The strains in the upper layer show initially positive values for the lower load levels, since here the load capacity of

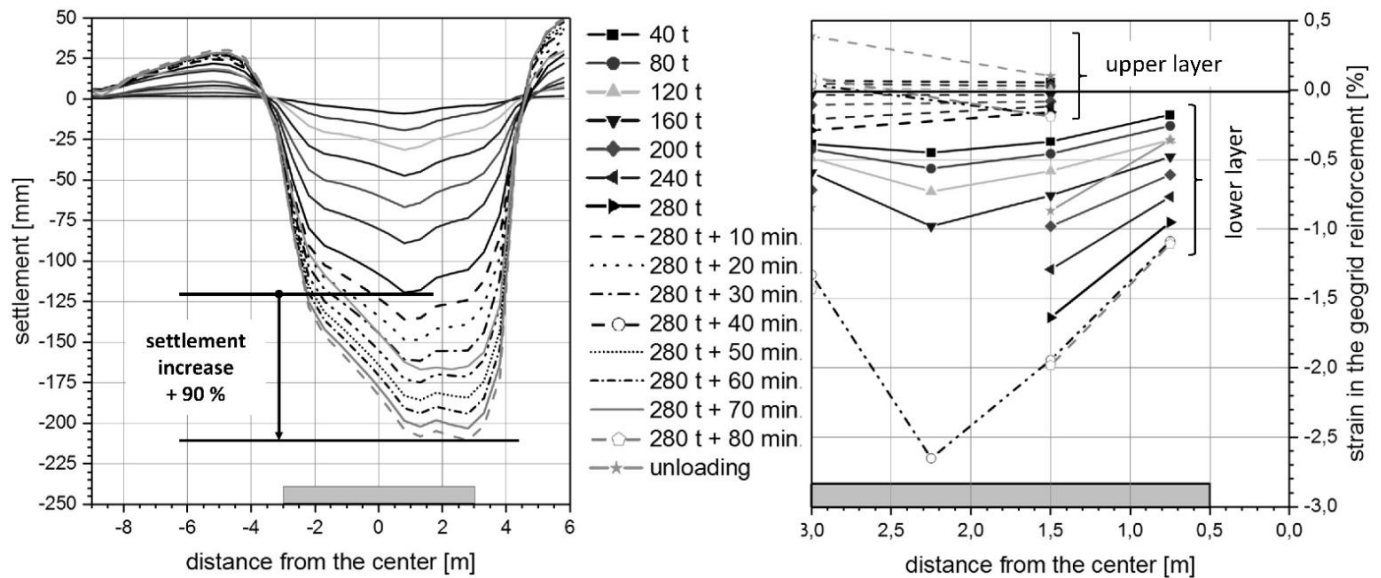


Figure 7. Measured settlement from the inclinometer chain along the y-axis (left), strain in both geogrid reinforcement layers along the x-axis (right).

the geogrid is not fully activated by deformations. When reaching the maximum load, the strains in the upper layer are about 5 to 25% of the values of the lower layer. Moreover, the measured strains of the geogrids do not behave proportionally to their tensile stiffness. This confirms the expectation of the increasing influence of the reinforcement effect in the lower part of the supporting layer. The missing measuring points result from failure values of the strain gages as a result of exceeding the maximum electric measuring range. Figure 7 shows the measurement results of the digital inclinometer chain. The setting of the soft layer in the middle axis of the crane mat is plotted for the respective loading steps. From about 160 t, unequal settlements of the crane mat can be observed. As the load increases, the crane mat starts tilting, while the settlement increases more and more per load step, which reveals a clear non-linearity in the load-bearing behavior. In addition, the elevations next to the crane mat can be clearly recognized as a result of the displacement of the soft layer due to undrained deformation behavior. The dashed curves show the deformation after reaching the maximum load of 280 t. Here, a strong time-dependent increase in deformation is observed, which leads approximately to a doubling of settlements to about 21.0 cm. Decisive for this is the consolidation of the almost water-saturated soft layer, which led to strong water leaks at the surface. After relieving the crane mat, uplifts of approximately 4.5 cm were set up in the center. In this case, the uplifts next to the crane mat after unloading are reduced again approximately to the values directly after the application of the maximum load, which shows that the deformations are predominantly volume constant changes in shape.

5 GROUND PRESSURE DISTRIBUTION UNDER TRACKED CONSTRUCTION MACHINERY

Within the framework of the research project, an elaborated field test was carried out to determine the ground pressure distribution under tracked plants resulting from the interaction behavior between construction machinery and the subgrade under site conditions. Figure 9-c shows the tested mobile crawler crane, here a Liebherr LR 11000 crane, which was subjected to different loading conditions. To measure the ground pressure, 13 earth pressure cells were placed under the crawler chassis. To protect the earth pressure cells from mechanical damage and to ensure a consistent stress distribution on the pressure pad, they were embedded with fine sand in a depth of 0.35 m. Furthermore, the settlement of the crawler undercarriage and in the subgrade at the level of the earth pressure sensors.

5.1 Analytical approach

In analytical approaches according to German Standard DIN EN 16228, ideally rigid undercarriages and support surfaces are assumed for the calculation of the contact pressure distribution under tracked construction machinery. This has the consequence that the determined ground pressure distribution has a constant or linear shape, similar to the stress distribution under eccentric loaded foundations. With increasing overturning moments under constant vertical forces the ground pressure at the tip of the track increases strongly,

while the pressures at the tail decrease. The stability of the plant can be increased by reducing the eccentricity of the center of gravity by vertical loading and retentive moments from central ballasts and counterweights. This idealized assumption of stability and ground pressure analysis for tracked plants lacks the consideration of the stiffness ratio between undercarriage and the subgrade, as well as nonlinear elastoplastic behavior of soil in general.

5.2 Results

The measured ground pressure distributions in Figure 8-a show a nonlinear envelope with pressure concentrations at the quarter points and a pressure minimum at the middle of the track. For the load case LC 6, with no eccentricity the ground pressure distribution becomes symmetrical. As the overturning moment increases in load case LC 7a, the ground pressure also increases in the front area of the track, while the ground pressure at the rear area is decreased. The shape of the curve still shows local maxima at the quarter points but generally higher values at the front. In comparison to the analytically determined ground pressures (blue line), which are considered under a load distribution angle of 45 ° at the level of the earth pressure transducers (dashed line), the measured ground pressures have significantly higher values. The consequence of this is local yielding and additional deformations in these areas, which further increase the differential settlement of the crawler of the construction machinery. This in turn causes additional tilting of the undercarriage and the whole superstructure, what leads to additional increasing of the overturning moments due to the increasing eccentricity of the center of gravity. These non-linear effects result in a significant negative influence on the stability of mobile construction machinery, which is not considered in calculations so far.

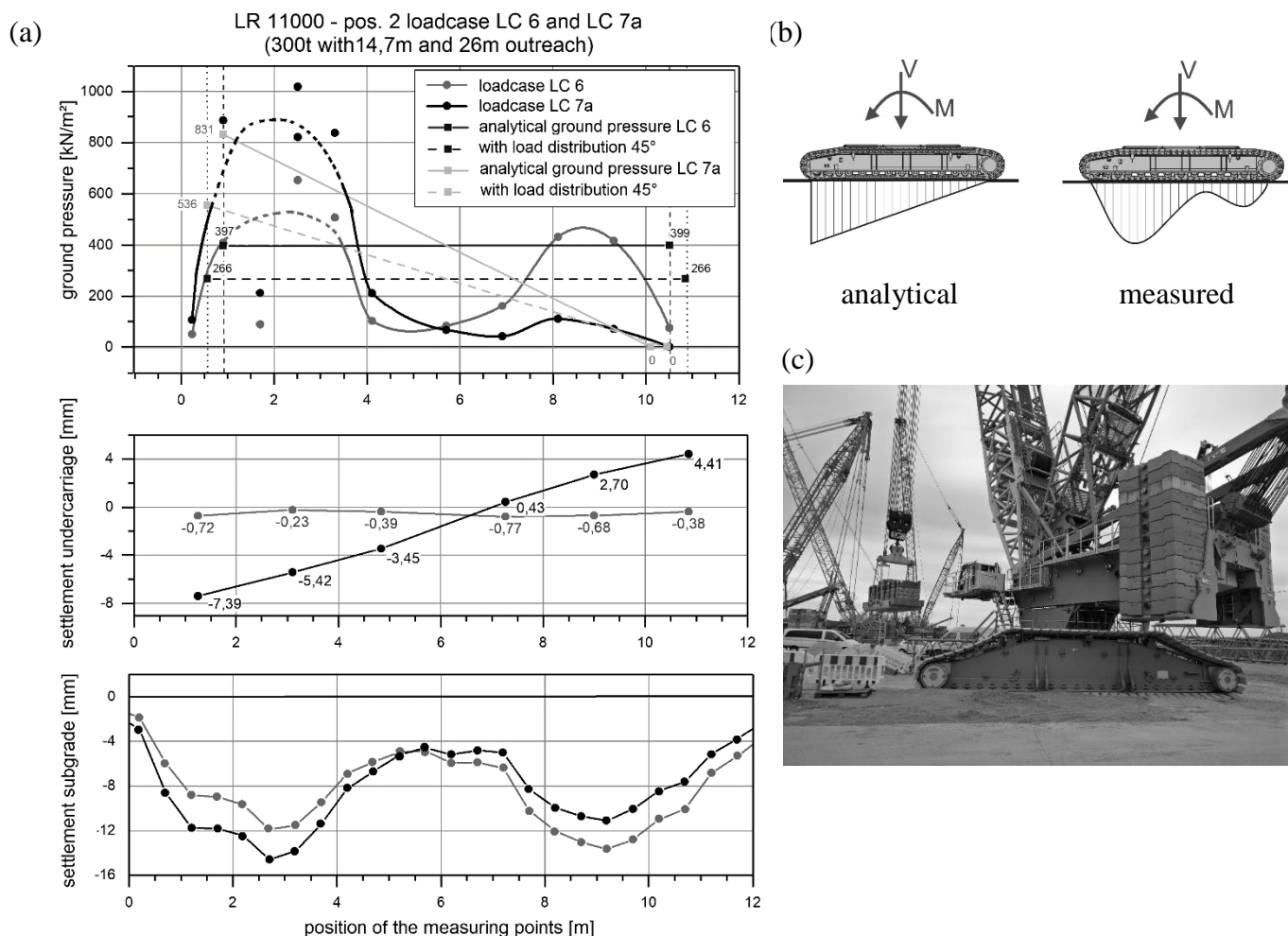


Figure 8. Measured ground pressure and settlements for the load cases LC 6 and LC 7a (a), schematic comparison between analytical und measured ground pressure distribution (b), crawler crane under load- ing condition with rotation of the super-structure (c).

6 GUIDELINE

Results gained from the investigations are incorporated in the draft of the "Recommendation for the Design and Execution of Working Platforms for Mobile Construction Machines and Crane Areas", which is intended to optimize the dimensioning of working platforms both technically and economically. The recommendation should serve as a basis for the dialogue between operators of mobile construction machinery and construction companies. Currently there exists no adequate basis for this important interface function. The research project is intended to make a contribution in order to close gaps in existing regulations and thus to improve the equipment and work safety of mobile construction machines and to avoid serious work accidents. The main content is the determination of design relevant load cases for different types of construction machinery, the development of an adequate design approach for unreinforced, single-layer-reinforced and multi-layer-reinforced supporting layers and to select simplified settlement calculation procedures to predict differential settlements.

7 CONCLUSION

The results of the model and field tests show that reinforcement with geosynthetics improves the load distribution in the subsoil and thus results in a more uniform distribution on the soft layer. The reinforcement contributes significantly to increase the bearing capacity and the stiffness of the supporting layers and thus to increase the stability of mobile construction machines. In addition, the reinforcement improves the deformation behavior mainly at higher load levels, as a result of the increasing activation of the geogrid. The failure mechanism of unreinforced base course systems consists of a combination of punching through the aggregate layer and punching shear failure of the soft layer. In the reinforced system the punching failure of the aggregate layer is mostly prevented and the punching shear failure of the soft layer needs a much higher loading level to be triggered as a result of the additional load distribution from the reinforcement due to the additional lateral restraint and the tensile membrane effect. While the lateral support by the reinforcement already works with very small deformations, the tensile membrane effect of the reinforcement requires a certain amount of vertical deformation to activate tensile forces in the reinforcement. In further course of the research project, additional field tests are planned to measure the ground pressures under crawler tracks and outriggers, as well as to measure the interaction between construction machinery and reinforced base courses. Furthermore, the effects of the operating states of mobile construction machinery on the load-bearing and deformation behavior of reinforced supporting layers are to be investigated.

REFERENCES

- BRE - Building Research Establishment 2004/2007. Working platforms for tracked plant: good practice guide to the design, installation, maintenance and repair of ground-supported working platforms (BR 470). IHS BRE Press, Bracknell, Berkshire, ISBN 186081 7009.
- German Geotechnical Society 2010. Recommendations for Design and Analysis of Earth Structures using Geosynthetic Reinforcements – EBGEO, 2nd Edition, Berlin: Ernst & Sohn.
- German Institute for Standardization 2006. DIN 4017:2006-03 Subsoil – Bearing capacity calculation for shallow foundations
- Giroud, J.-P. & Noiray, L. 1981. Geotextile-Reinforced unpaved road design. Journal of the Geotechnical Engineering Division Vol. 107 (No. GT9), pp. 1233–1254.
- Meyerhof, G. G. 1974: Ultimate bearing capacity of footings on sand layer overlying clay. Canadian Geotechnical Journal Vol. 11 (No. 2.): pp. 223–229.
- Kleih, J. et. al. 2009. Requirements for the working platforms to ensure the stability of special heavy construction machinery (German). BauPortal, Vol. 9/2009, pp. 499-503.
- Lehn, J., Moormann, C. 2017. Investigations on a geosynthetic reinforced bearing layer under static and cyclic loading. Proceedings of the 19th International Conference on Soil Mechanics and Geotechnical Engineering, , pp. 1841-1844, Seoul, Korea.
- Moormann, C., Lehn, J., Tazl, M., Worbes, R., 2017. Measuring of the load bearing and deformation behavior of a working platform for mobile cranes in a wind park (German). 15. Information and Presentation Meeting about Synthetics in Geotechnical Engineering (15. Informations und Vortragstagung Kunststoffe in der Geotechnik), pp. 564-569, Würzburg, Germany